INFLUENCE OF PARTICLE SIZE AND HYDROCOLLOID TYPE ON LIPID DIGESTION OF THICKENED EMULSIONS

Article *in* Food & Function · June 2020

DOI: 10.1039/D0FO01202E

4 authors, including:

Paz Robert
University of Chile
90 PUBLICATIONS **2,146** CITATIONS
SEE PROFILE

Elizabeth Troncoso
Universidad Tecnológica Metropolitana
37 PUBLICATIONS **844** CITATIONS
SEE PROFILE

Carla Arancibia
University of Santiago, Chile
17 PUBLICATIONS **200** CITATIONS
SEE PROFILE

Food & Function

ROYAL SOCIETY OF CHEMISTRY

PAPER

View Article Online
View Journal

Cite this: DOI: 10.1039/d0fo01202e

Influence of the particle size and hydrocolloid type on lipid digestion of thickened emulsions

N. Riquelme,[a,b] P. Robert,[b] E. Troncoso[c,d] and C. Arancibia *[a]

Received 9th May 2020,
Accepted 11th June 2020

DOI: 10.1039/d0fo01202e

rsc.li/food-function

Hydrocolloids are used as stabilizing agents in order to enhance the physical stability of emulsions during their storage. However, they can also play an important role in nutrient release and bioavailability. In this context, the aim of this research was to study the effect of the emulsion type and thickener type on the physical–structural changes and free fatty acid release during *in vitro* digestion. Oil-in-water emulsions were prepared with different particle sizes (CE: conventional emulsions and NE: nanoemulsions) and thickening agents (starch and xanthan gum). The experimental conditions of homogenization used allowed food emulsions to be obtained at the microscale and nanoscale, with particle sizes ranging among 3.2–3.4 μm and 78–107 nm for CE and NE, respectively. The addition of thickening agents (XG and ST) modified the physical properties of emulsions (particle size, zeta potential and stability) slightly, and thickened samples with similar viscosity were obtained. The kinetics of FFAs released during the *in vitro* intestinal digestion showed no significant differences ($p > 0.05$) in the digestion rate among samples; however, emulsion and thickener types decreased the final extent of free fatty acids, being more evident for those samples with starch. Xanthan gum kept the particle size of nanoemulsions stable during the oral and gastric phases, which promoted the release of FFAs during the intestinal phase. Therefore, xanthan gum could be used as a thickening agent of nanoemulsions exerting a minor impact on their lipid bioaccessibility.

1. Introduction

The increasing elderly population (>60 years) in the world has led the food industry to design products according to their nutritional needs, in particular to maintain this population's health and quality of life. This group of people has a high risk of nutritional deficiencies and/or chronic disease because of the many changes (physiological, psychological and social) they experience as a consequence of aging.[1–3] Recently, some strategies for designing products focused on nutrition for elderly people have been proposed.[3–6] These consist of the development of functional foods with enhanced bioaccessibility of essential nutrients and/or bioactive compounds based on more efficient nutrient delivery systems, such as nanoemulsions.[7–9] Furthermore, older people often have reduced masticatory activity[3] and/or suffer from swallowing disorders, such as dysphagia, which can lead to malnutrition and/or pneumonia by aspiration.[5,10] In order to minimize these difficulties, food texture can be modified by the incorporation of hydrocolloids, which can improve the swallowing process, making it safer and more efficient.[4,11–14] Thus, the use of both nanoemulsions and hydrocolloids will be considered in this study.

Oil-in-water (O/W) nanoemulsions are a dispersion of two immiscible liquids, where the lipid phase is dispersed into an aqueous phase in the form of small oil droplets (<100 nm).[15] Because of their ability to increase the bioavailability of lipid compounds, these systems have been studied extensively. Compared with nanoemulsions, conventional emulsions (large particle size) are not so effective at delivering bioactive ingredients during digestion.[16] Nanoemulsions' advantage relies on their larger surface area (small oil droplets) in contact with digestive enzymes such as lipase, allowing a higher release of lipid compounds, which can be incorporated into mixed micelles, structure that corresponds to their more bioaccessible form.[17] However, there are several factors that influence nanoemulsion digestion within the gastrointestinal tract, such as the particle size, interfacial properties and structure, rheological properties and/or texture, among others.[14,18,19] Therefore, it is important to understand how physical and microstructural properties of nanoemulsions are modified during gastrointestinal tract digestion, in order to design more bioaccessible

[a]*Departamento de Ciencia y Tecnología de los Alimentos, Facultad Tecnológica, Universidad de Santiago de Chile, Obispo Umaña 050, Estación Central, Chile. E-mail: carla.arancibia@usach.cl; Tel: +56227184518*
[b]*Departamento de Ciencia de los Alimentos y Tecnología Química, Facultad de Ciencias Químicas y Farmacéuticas, Universidad de Chile, Santos Dumont 964, Independencia, Chile*
[c]*Departamento de Química, Facultad de Ciencias Naturales, Matemática y del Medio Ambiente, Universidad Tecnológica Metropolitana, Las Palmeras 3360, Ñuñoa, Chile*
[d]*Programa Institucional de Fomento a la Investigación, Desarrollo e Innovación, Universidad Tecnológica Metropolitana, Ignacio Valdivieso 2409, San Joaquín, Chile*

nanoemulsions that promote health status and consumers' nutrition.

There are several thickening agents that can be used to treat dysphagia, such as Enterex® (Victus Inc.), Nat100® (Laboratorio Boston S.A); Vegenat® (Nutrisens Group) based on modified starch; Thick & Easy® (Hormel Foods™); Vivalite® Thickener Plus (Renova Functionals S.A) based on modified starch and maltodextrin; Resource® Clear (Nestlé S. A.) and Font Activ® Espesante Claro (Ordesa©) based on xanthan gum. Starch has been traditionally used as a thickener for dysphagia patients because it can be used to modify fluid viscosity without producing major changes in the organoleptic properties.[20] However, the viscosity of food products that have been thickened with starch can change during oral processing,[21] since salivary α-amylase breaks down the chains of amylose and amylopectin. This fact leads to a considerable decrease in viscosity in the mouth, which may be unsafe to dysphagia patients.[22,23] Therefore, non-starch-based hydrocolloids can be used as food thickening agents as an alternative to starch. Xanthan gum is a polysaccharide produced by *Xanthomonas campestris.*[24] It presents great stability under a wide range of temperatures and pH levels.[25] It is used in the food industry as a thickener due to its palatability and smooth texture.[12] In addition, this hydrocolloid is characterized by its resistance to enzymatic degradation during oral processing. This represents an advantage to dysphagia patients, because in the presence of saliva, it does not become thinner over time.[26]

In the case of emulsions, hydrocolloids are used as stabilizing or emulsifying agents because some of them have surface activity, presenting polar and nonpolar groups that allow the reduction of interfacial tension at the oil–water interface.[27] In addition, hydrocolloids improve the physical stability of emulsions by inducing the formation of a thick hydrophilic coating around oil droplets, which can promote electrostatic and steric repulsion among them.[15,28] However, the impact of hydrocolloids on lipid digestion is not well documented. Chang & McClements[29] reported that the use of an anionic polysaccharide (fucoidan) increased the initial digestion rate of fish oil emulsions stabilized by protein, due to its ability to prevent lipid droplet aggregation, thereby increasing the lipids' surface area available for lipase. Xu *et al.*[30] studied *in vitro* the effect of two anionic polysaccharides (pectin and xanthan gum) on the lipid digestion of fish-oil-in-water emulsions. The results suggested that the incorporation of anionic polysaccharides promoted lipid digestion. However, Qin *et al.*[31] and Arancibia *et al.*[32] demonstrated that the use of hydrocolloids, such as cationic chitosan and anionic alginate and carboxymethyl cellulose, respectively, decreased the rate and final extent of free fatty acids released during the *in vitro* lipid digestion of food emulsions/nanoemulsions. These hydrocolloids caused physical retention of oil droplets into the aqueous phase, retarding the lipase access to the substrate or inhibiting lipid digestion.

Against this background, we hypothesized that microstructural differences of thickened emulsions could modify the free fatty acids released during the *in vitro* digestion of these food matrices, affecting consequently lipid bioaccessibility. The aim of this research was to study the impact of the emulsion type (conventional emulsion *vs.* nanoemulsion) and thickener type (starch or xanthan gum) on the physical–structural changes and free fatty acids released during *in vitro* digestion.

2. Materials and methods

2.1 Materials

Avocado oil (Casta de Peteroa – Terramater S.A., Chile), soy lecithin (Metarin P, Cargill, Blumos S.A., Chile), Tween 80 (Sigma-Aldrich S.A., USA), a starch-based thickener (ENTEREX®, Victus Inc., USA), a xanthan gum-based thickener (RESOURCE® CLEAR, Nestlé Health Science S.A., France) and purified water (from an inverse osmosis system, Vigaflow S.A., Chile) were used to prepare emulsions. Pepsin from porcine gastric mucosa (3200–4500 units per mg protein, P6887), pancreatin from porcine pancreas (4 × USP specifications, P1750), bile extract (from porcine, B8631) and lipase from porcine pancreas (100–500 units per mg protein using olive oil, L3126) purchased from Sigma-Aldrich (USA), and different salts (KCl, KH_2PO_4, $NaHCO_3$, NaCl, $MgCl_2(H_2O)_6$, $(NH_4)_2CO_3$, NaOH, HCl and $CaCl_2(H_2O)_2$) purchased from Merck (Germany) and Winkler (Chile) were used to prepare simulated digestion fluids. Nile Red (Sigma-Aldrich S.A., USA) and polyethylene glycol (Sigma-Aldrich S.A., USA) were used in microscopy analyses.

2.2 Thickened emulsion preparation

Different O/W emulsions were prepared with varying particle sizes (conventional emulsion-CE and nanoemulsion-NE) and thickener types (starch-ST or xanthan gum-XG). Two control samples with no-added thickeners but with different particle sizes (CE and NE) were prepared. All emulsions contained 5% w/w of avocado oil (lipid phase), 6% w/w of a mixture of emulsifiers (5% w/w soy lecithin and 1% w/w Tween 80) and 89% w/w of purified water (aqueous phase). For CE elaboration, the lipid phase was dispersed into the aqueous phase (water and emulsifier mixture) using a high-speed homogenizer (IKA T25, Ultra Turrax, Germany) at 10 000 rpm for 15 min. The pre-emulsion was homogenized by high pressure (APV 2000, SPX Flow, Poland) using the following operation conditions: 1 cycle at 100 bar- and 9 cycles at 1500 bar to CE and NE, respectively. Thickeners were then added to the emulsions at iso-viscous concentrations (4.45 g of ST or 3.2 g of XG for 100 g of CE, and 5 g of ST or 4 g of XG for 100 g of NE) using a kitchen robot (Thermomix™ TM5, Vorwerk Elektrowerke GmbH & Co, Germany) at 60 °C and 500 rpm for 10 min. These food emulsions were stored in glass flasks at 4 °C for 24 h before measurements were performed.

2.3 Characterization of thickened emulsions

2.3.1 Particle size and zeta potential. The particle size (Sauter diameter $D_{3,2}$) of conventional emulsions was determined by optical microscopy, where 5–6 images of each

sample were captured with a digital camera (EOS Rebel T3, Canon, Japan) connected to an optical microscope at 100× (PrimoStar, Carl Zeiss, Germany), and then processed with AxioVision software (AxioVision Rel. 4.8, Carl Zeiss, Germany) to calculate the average diameter of at least 200 oil droplets (from each replica) following eqn (1).

$$D_{3.2} = \frac{\sum n_i d_i^3}{\sum n_i d_i^2} \quad (1)$$

where d_i is the oil droplet diameter and n_i is the number of droplets having a diameter d_i. The particle size distribution of the emulsions was determined as a frequency distribution through histogram analysis.

The particle size (hydrodynamic diameter) of nanoemulsions was determined by dynamic light scattering (Nano ZS, Malvern Instruments, UK) using a refractive index value of 1.47 for the disperse phase (avocado oil) and of 1.33 for the continuous phase (water). Samples were diluted to 6% v/v using Milli-Q water to obtain a solution without turbidity. Each value of the particle size corresponds to an average of three measurements of the hydrodynamic diameter of the same sample.

The zeta potential (ZPot) of all emulsions was measured by Electrophoretic Light Scattering (ELS) using Zetasizer equipment (Nano ZS, Malvern Instruments, UK). For these analyses, samples were diluted to 6% v/v using Milli-Q water to obtain a solution without turbidity. A refractive index of 1.47 for avocado oil was used for the measurements. The ZPot values correspond to an average of 3 measurements for each sample.

2.3.2 Flow behavior. Flow behavior of the emulsions was determined by using a rotational rheometer (RheolabQC, Anton Paar, Austria) equipped with double gap or concentric cylinder geometry (DG42 and CC27 for control samples and thickened emulsions, respectively). Shear stress was recorded at a shear rate between 1 and 200 s^{-1} and 200 and 1 s^{-1} for 120 s. The equipment worked at 37 ± 1 °C. The temperature was controlled using a Peltier system. The emulsions were allowed to stand for 10 min before measurements were conducted, to recover the emulsion structure and reach the test temperature. The upward flow curves of control and starch-based samples were fitted to the Ostwald-de Waele model (eqn (2)), and xanthan gum-based emulsions to the Herschel–Bulkley model (eqn (3)).

$$\sigma = K\dot{\gamma}^n \quad (2)$$

$$\sigma = \sigma_0 + K\dot{\gamma}^n \quad (3)$$

where σ is shear stress (Pa), σ_0 is yield stress (Pa), K is the consistency index (Pa s), $\dot{\gamma}$ is the shear rate (s^{-1}) and n is the flow index. Also, the thixotropic behavior of different emulsions was determined by the percentage of the relative hysteresis area (eqn (4)):[33]

$$A_r = \frac{A_{up} - A_{down}}{A_{up}} \times 100 \quad (4)$$

where A_r is the percentage of the relative hysteresis area, A_{up} is the area under the upstream data point curve and A_{down} is the area under the downstream data point curve.

All measurements were carried out in triplicate and each replica was measured twice (6 measurements in total). Apparent viscosity at a shear rate of 50 s^{-1} ($\eta_{50\ s^{-1}}$) was used as a parameter of comparison between samples. This shear rate was chosen because it is taken to be the shear rate that occurs during the food swallowing process.[34]

2.3.3 Physical stability. The physical stability of the thickened emulsions was evaluated through a creaming index (CI) after a centrifugation process. Hence, 8 mL of each emulsion were placed in conical centrifuge tubes and then were centrifuged (Universal 32R, Hettich, UK) at 2400*g* for 15 min in order to accelerate physical destabilization of the emulsions.[35] Then, the CI was calculated using eqn (5):

$$CI(\%) = \frac{H_S}{H_E} \times 100 \quad (5)$$

where H_E is the total height of the emulsion and H_S is the height of the cream layer formed.

2.4 *In vitro* lipid digestion

Emulsions (CE and NE) were subjected to *in vitro* lipid digestion to evaluate the influence of the emulsion particle size and thickener type on the physical properties, microstructure and free fatty acid (FFA) release. Mouth, stomach and intestinal fluids were prepared according to the standardized protocol INFOGEST 2.0[36] with some modifications, to carry out simulated static *in vitro* gastrointestinal food digestion.

2.4.1 Mouth phase. 25 g sample (preheated to 37 °C) were mixed with 25 mL human saliva (1 : 1) and incubated at 37 °C for 2 min in an incubator shaker at 80 rpm (NB-205, N-Biotek INC., Korea). Human saliva was obtained from a single healthy volunteer, who did not consume food 2 h before saliva collection. First, the volunteer rinsed his mouth with water and then spat saliva for a period of 2 h. The saliva was then placed in a glass beaker under an ice bath. Saliva collection was performed in accordance with the guidelines approved by the ethics committee at the University of Santiago of Chile (Report no. 705). Informed consent was obtained from the human participant of this study.

2.4.2 Stomach phase. The simulated gastric fluid (SGF) consisted of an electrolyte stock gastric solution (1.7% v/v 0.5 M KCl, 0.2% v/v 0.5 M KH_2PO_4, 3.0% v/v 1.0 M $NaHCO_3$, 3.0% v/v 2.0 M NaCl, 0.1% v/v 0.15 M $MgCl_2(H_2O)_6$, 0.2% v/v 0.5 M $(NH_4)_2CO_2$, 0.3% v/v 6.0 M HCl, 0.001% v/v 0.3 M $CaCl_2$, and 91.5% v/v purified water) and pepsin solution (0.5% w/v in purified water). At this stage, 50 mL of the *in vitro* oral digested sample (bolus) was mixed with 50 mL of SGF (ratio 1 : 1) preheated at 37 °C. Then, the mixture was incubated in a water bath (WNB7, Memmert GmbH+Co, Germany) at 37 °C for 1.5 h under continuous agitation at 200 rpm. The pH of the mixture was monitored and controlled using an automatic titration unit (902 Titrando, Metrohm, USA) equipped with Tiamo 2.4 software. To adjust gastric pH, 0.5 M HCl solution

was used until the conditions of the human stomach during digestion were reached (pH 2.0), following three control stages: (1) pH 4.0, adding 0.1 mL min^{-1} for 15 min; (2) pH 3.0, adding 0.08 mL min^{-1} for 35 min; and (3) pH 2.0, adding 0.07 mL min^{-1} for 40 min.

2.4.3 Intestine phase. The simulated intestinal fluid (SIF) was prepared with electrolyte stock intestinal solution (1.7% v/v 0.5 M KCl, 0.2% v/v 0.5 M KH_2PO_4, 10.5% v/v 1.0 M $NaHCO_3$, 2.4% v/v 2.0 M NaCl, 0.2% v/v 0.15 M $MgCl_2(H_2O)_6$, 0.15% v/v 6.0 M HCl, 0.01% v/v 0.3 M $CaCl_2$ and 85% v/v purified water), bile salt solution (7% w/v in stock intestinal solution), pancreatic dispersion (0.003% w/v in stock intestinal solution) and lipase solution (10% w/v in stock intestinal solution). First, 100 mL of the mixture obtained from the stomach phase (chyme) was mixed with 100 mL of SIF (ratio 1 : 1), adjusting the pH to 7.0 with 0.5 M NaOH solution. This mixture was incubated at 37 °C for 2 h and stirred at 200 rpm, maintaining its pH at 7.0 by adding 0.5 M NaOH solution (0.5 M) with the help of the pH-stat device (902 Titrando, Metrohm, USA). This was carried out to neutralize the FFAs generated by lipolysis during the lipid digestion process. The amount of FFAs released was calculated using the following eqn (6):[18]

$$\%\mathrm{FFA} = \left(\frac{V_{\mathrm{NaOH}(t)} \times M_{\mathrm{NaOH}} \times M_{\mathrm{w_{oil}}}}{m_{\mathrm{oil}} \times 2}\right) \times 100 \qquad (6)$$

where $V_{\mathrm{NaOH(t)}}$ corresponds to the volume (L) of NaOH solution used to neutralize the FFAs generated during the digestion time, M_{NaOH} is the molar concentration (mol L^{-1}) of the NaOH solution used to titrate the sample, $M_{\mathrm{w_{oil}}}$ is the molecular weight (g mol^{-1}) of the oil, and m_{oil} is the amount (g) of the initial oil present in the sample.

To compare the digestion kinetics of the different samples, the initial rate of FFAs released was calculated by data fitting to a linear regression during the first 25 min of *in vitro* intestinal digestion. The final digestion extent was calculated as the total percentage of FFAs released at the end of the *in vitro* intestinal digestion.

2.4.4 Microstructure. After each phase of digestion, the emulsion microstructure was observed by confocal laser scanning microscopy (CLSM) (LSM 510, Zeiss, Germany). First, 150 μL of samples from different digestion phases (before digestion and after digestion in each phase) were dyed with Nile Red solution (30 μL of 0.1 g L^{-1} in polyethylene glycol). Then, each sample-dye (10 μL) was placed between two coverslips in the observation chamber, using a 63X oil immersion objective lens. The excitation and emission wavelengths of Nile Red were 559 nm and 636 nm, respectively. For these microscopy analyses, at least 10 images of each sample were recorded and analyzed using ZEN Lite 2.3 software (Zeiss, Germany).

2.5 Statistical analysis

The experimental data were reported as the average of at least three replicates and their corresponding standard deviation. Two-way ANOVA (with the emulsion and thickener type as independent variables) and Tukey's test with a level of significance of $\alpha = 0.05$ were performed to identify significant differences among samples, using XLSTAT© software (Addinsoft, France).

3. Results and discussion

3.1 Initial characterization of the thickened emulsions

Emulsions at the micro-scale and nano-scale were produced with and without thickeners, applying different experimental conditions (high-speed and high-pressure homogenization, respectively). Table 1 shows the initial physical parameters of the thickened emulsions. The particle size was significantly higher ($p < 0.05$) in CE (3.17 to 3.37 μm) than in NE (78 to 107 nm) (Table 1), and the addition of hydrocolloids as a thickening agent slightly increased the particle size of both types of emulsions. This was more evident in emulsions thickened with xanthan gum (3.37 μm for CE and 107 nm for NE). An increase in the particle size may be due to the adsorption of xanthan gum at the oil–droplet interface. The anionic polysaccharide can be located at the oil–water interface and under this condition, it can interact with the other emulsifiers to form a thick emulsifier layer around oil droplets, which increased the particle size values of the emulsions.[37,38] Regarding zeta potential, all emulsions showed a negative electrical charge with values among −58.3 and −41 mV (Table 1). This is due primarily to the use of soy lecithin, an emulsifier negatively charged by the anionic phospholipids in its chemical structure.[39] In addition, conventional emulsions showed more electronegative ZPot values than nanoemulsions, probably because of the formation of lecithin micelles induced by an excess of this surfactant in the aqueous phase. A larger particle size of conventional emulsions implies a smaller interfacial area around oil droplets; therefore there will be soy lecithin molecules to adsorb at the oil–water interface and the other ones will be available to form micelles.[40] The thickener type also significantly affected ($p < 0.05$) the ZPot values, where the CE and NE samples with xanthan gum showed a more negative electrical charge than starch-based samples, due to the anionic groups in the xanthan gum chain.[38] Regarding the flow behavior study, emulsions with different concentrations of hydrocolloids but with similar apparent viscosity ($\eta_{50\ s^{-1}}$, Table 1) were obtained. This consideration was defined to obtain negligible distortion in the results of *in vitro* digestion assays by the effect of differences in the initial viscosity of samples. The flow curves for control and starch-based emulsions were fitted to the Ostwald-de Waele model ($R^2 > 0.99$). However, the flow curves for xanthan gum-based emulsions were fitted to the Herschel–Bulkley model ($R^2 > 0.98$) because these showed an initial resistance to flow (yield stress) (Table 1, Fig. 1). Control emulsions (without thickener) presented a Newtonian flow behavior (flow index ~1, Table 1), while thickened emulsions showed a pseudoplastic behavior (flow index < 1). Also, the thickened emulsions presented a thixotropic behavior showing differences between the emulsifier type, where emulsions with starch showed a greater thixotropic behavior (Table 1). The physical stability of emulsions

Table 1 Initial physical parameters of the thickened emulsions

Emulsion type	Thickener type	Particle size (nm)	Zeta potential (mV)	σ_0 (Pa)	K (Pa·s)	n	A_r (%)	$\eta_{50\ s^{-1}}$ (Pa·s)	Creaming index (%)
Conventional emulsion (CE)	No-added	3170 ± 90^{b}	-55.1 ± 3.2^{cd}	—	0.002 ± 0.001^{a}	1.00 ± 0.06^{c}	—	0.001 ± 0.0002^{a}	11.5 ± 1.8
	Starch	3166 ± 90^{b}	-51.9 ± 1.8^{c}	—	3.691 ± 0.484^{c}	0.53 ± 0.01^{b}	8.93 ± 0.71^{b}	0.556 ± 0.003^{b}	n.o
	Xanthan gum	3368 ± 78^{b}	-58.3 ± 3.5^{d}	20.2 ± 0.6^{a}	2.265 ± 0.114^{b}	0.37 ± 0.03^{a}	5.00 ± 0.85^{a}	0.559 ± 0.006^{b}	n.o
Nanoemulsion (NE)	No-added	78 ± 1.0^{a}	-44.0 ± 0.4^{ab}	—	0.001 ± 0.001^{a}	1.00 ± 0.02^{c}	—	0.001 ± 0.0003^{a}	n.o
	Starch	86 ± 0.4^{a}	-41.0 ± 2.3^{a}	—	3.736 ± 0.248^{c}	0.53 ± 0.01^{b}	16.29 ± 1.68^{c}	0.548 ± 0.011^{b}	n.o
	Xanthan gum	107 ± 8.0^{a}	-50.8 ± 2.1^{bc}	22.0 ± 1.0^{a}	1.837 ± 0.507^{b}	0.41 ± 0.03^{a}	5.58 ± 1.18^{a}	0.565 ± 0.002^{b}	n.o

Notes: 1. Different letters indicate significant differences ($p < 0.05$) in the parameters (same column) for different thickened emulsions. 2. Flow curves were fitted to the Ostwald-de Waele model ($R^2 > 0.99$) for emulsions without thickener and starch-based emulsions, and the Herschel–Bulkley model ($R^2 > 0.98$) for xanthan gum-based emulsions. σ_0: yield stress, K: consistency index, n: flow index, A_r: hysteresis area and $\eta_{50\ s^{-1}}$: apparent viscosity at 50 s^{-1}. n.o: not observed.

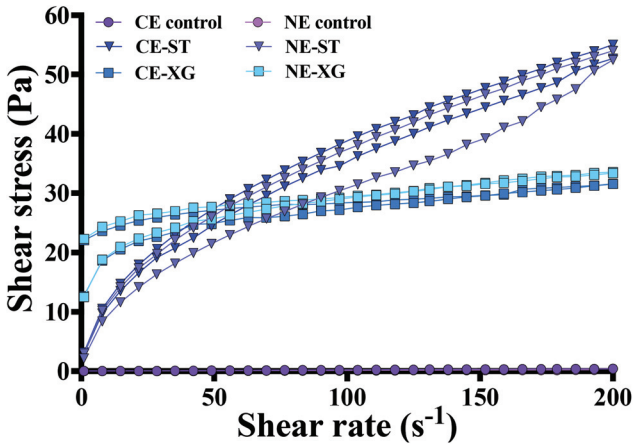

Fig. 1 Flow curves (upward and downward curves) of thickened emulsions. CE: conventional emulsion, NE: nanoemulsion, control: without thickener, ST: starch and XG: xanthan gum. Flow curves were fitted to the Ostwald-de Waele model ($R^2 > 0.99$) for emulsion control and starch-based emulsions, and the Herschel–Bulkley model ($R^2 > 0.98$) for xanthan gum-based emulsions.

was monitored by creaming formation after a centrifugation process. All samples presented a good physical stability. No signs of destabilization were detected (Fig. 2), except for the CE-control (without thickener), which showed the formation of a cream layer on the top of the tube, corresponding to 11.5% of the creaming index (Table 1). The stability of emulsions depends on several factors. These include the particle size, since it is known that an emulsion with large droplets (conventional emulsions) is less stable than the one with small droplets (nanoemulsions) and the addition of a thickening agent decreases the destabilization rate of emulsions, because it increases the viscosity of the continuous phase.[15] Therefore, we can conclude that good physical stability can be induced in emulsions by both factors: particle size and the addition of thickening agents (starch and xanthan gum).

3.2 *In vitro* lipid digestion

The kinetics of free fatty acid (FFA) release in conventional emulsions (CE, CE-ST and CE-XG) and nanoemulsions (NE, NE-ST and NE-XG) during *in vitro* intestinal digestion is shown in Fig. 3, where two regions can be clearly distinguished. In the first region, %FFAs released rapidly increased with increasing digestion time (25 min), due to the fast adsorption of the lipase at the oil droplet surface.[41] In the second region, FFAs released reached constant values and did not increase with digestion time, because the lipolysis products (*i.e.* fatty acids and monoglycerides) compete with lipase for the available surface area in the oil–water interface, reducing its activity.[42] Also, differences among emulsions in the amount of FFAs released at the end of the intestinal digestion were found, where conventional emulsions showed a lower FFA release (30–43%) than nanoemulsions (43–60%). This behavior agrees with the studies conducted by Majeed *et al.*,[43] Zhang *et al.*[44] and Salvia-Trujillo *et al.*,[45] who reported that emulsions with a small particle size (nano-scale) were digested more rapidly than the large ones (micro-scale), due to the increased area of the oil droplet exposed to the enzyme action. Moreover, the addition of either a CE or NE thickener (ST or XG) decreased the release of FFAs with respect to the control one (CE or NE). This tendency was more evident for those samples with the largest particle size (conventional emulsions) (Fig. 3). Hydrocolloids in the aqueous phase of o/w emulsions can: (i) modify the properties of the oil droplet interface and the viscosity of the continuous phase, (ii) interact with other components (*e.g.* ions, bile salts and enzymes), and (iii) generate changes in the physicochemical properties of the gastrointestinal fluids. All these factors could impact the digestion kinetics of thickened emulsions.[29,46,47]

Table 2 shows the FFA digestion rate and FFA release from the oil-in-water emulsion with and without thickeners during the *in vitro* intestinal digestion. There were no significant differences ($p > 0.05$) in FFA digestion rates between emulsions (~ 3.3% FFA per min), while the %FFAs released at the end of digestion varied significantly ($p < 0.05$) depending on the particle size and thickener type (Table 2). Nanoemulsions showed significantly higher ($p < 0.05$) FFAs released with respect to conventional emulsions, regardless of the thickener type, which can be attributed to the greater interfacial area that facilities the substrate-enzyme interaction.[44,45,48,49] The thickener type significantly affected ($p < 0.05$) the final amount of FFAs obtained (Table 2), although its effect was different according to the scale of the emulsions (micro or nano-scale).

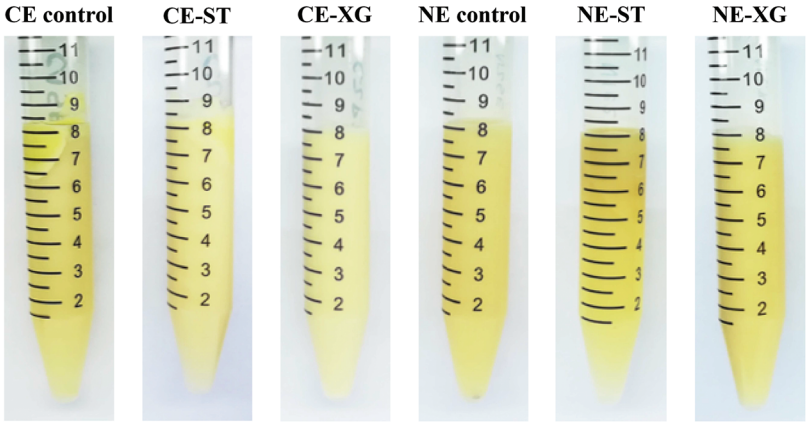

Fig. 2 Physical stability of the thickened emulsions after the centrifugation process. CE: conventional emulsion, NE: nanoemulsion, control: without thickener, ST: starch, and XG: xanthan gum.

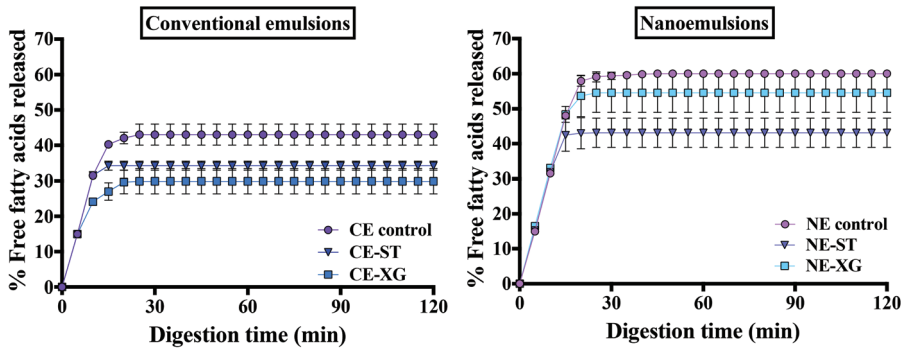

Fig. 3 Free fatty acids released during the *in vitro* intestinal digestion of the thickened emulsions elaborated with different emulsions and thickener types. CE: conventional emulsion, NE: nanoemulsion, control: without thickener, ST: starch, and XG: xanthan gum.

Table 2 Digestion rate and final extent of free fatty acids (FFA) released from the thickened emulsions during the *in vitro* intestinal digestion

Emulsion type	Thickener type	Digestion rate (% FFA per min)	Final extent (FFA released %)
Conventional emulsion (CE)	No-added	3.305 ± 0.0001^{a}	43.1 ± 3.0^{bc}
	Starch	3.305 ± 0.0007^{a}	34.2 ± 1.3^{ab}
	Xanthan gum	3.302 ± 0.0007^{a}	29.8 ± 3.6^{a}
Nanoemulsion (NE)	No-added	3.306 ± 0.0004^{a}	60.1 ± 0.2^{d}
	Starch	3.305 ± 0.0017^{a}	43.2 ± 4.2^{c}
	Xanthan gum	3.306 ± 0.0004^{a}	54.6 ± 5.6^{cd}

Note: 1. Different letters indicate significant differences ($p < 0.05$) in the parameters (same column) for different thickened emulsions.

In the case of CE thickened with xanthan gum, the release of FFAs decreased significantly in comparison with control samples (CE). However, when this hydrocolloid was added into nanoemulsions, no significant differences ($p > 0.05$) were found between control NE and xanthan gum-based NE, indicating a minor impact of this thickening agent on lipid bioaccessibility. This behavior can be influenced by the formation of a compact and stable network structure around the oil droplets that protects them against coalescence, maintaining a relatively small particle size during the oral and gastric digestion phases.[50] The addition of starch to NE decreased significantly the FFAs released, which may be due to the lower stability of this sample under mouth and gastric digestion conditions, which increased its particle size, consequently reducing the production of FFAs during the *in vitro* intestinal digestion. Therefore, FFA release decreased significantly in xanthan gum-based CE and starch-based NE.

3.3 Physical changes of thickened emulsions during their *in vitro* lipid digestion

The particle size and the microstructure of the emulsions after each *in vitro* digestion phase (mouth, stomach and intestines) were characterized to obtain information about how these physical properties are affected by digestive action. Fig. 4 shows the changes in the particle size of the different emulsions after the oral phase, where a significant increase ($p < 0.05$) in the particle size (PS) was found, except for the XG-based nanoemulsion. This result was in line with a shift in the particle size peak towards higher values (Fig. 5) with respect to the control peak and with microstructure photographs (Fig. 6). Therefore, mouth digestion led to an increase in the particle population with larger sizes, due to coalescence of oil droplets

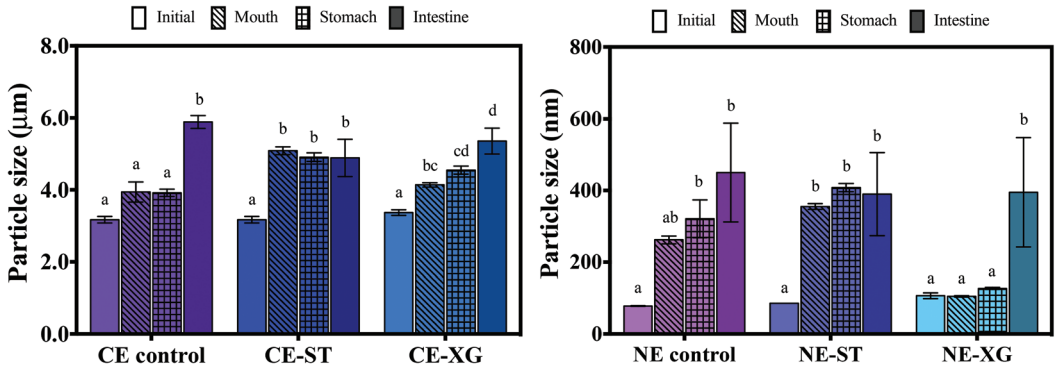

Fig. 4 Changes in the mean particle size of the thickened emulsions after each phase of the *in vitro* digestion. CE: conventional emulsion, NE: nanoemulsion, control: without thickener, ST: starch, and XG: xanthan gum. Different letters indicate significant differences ($p < 0.05$) between the *in vitro* digestion stages for each thickened emulsion.

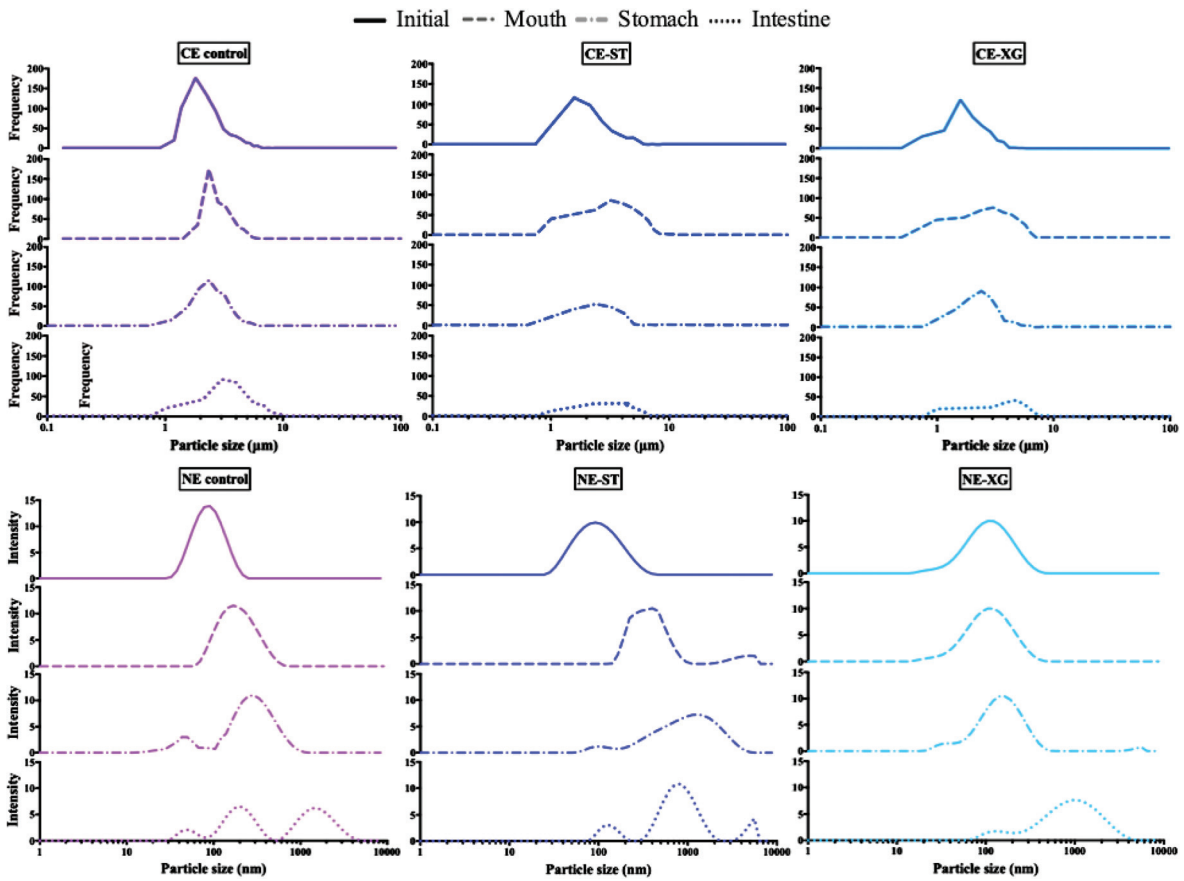

Fig. 5 Changes in the particle size distribution of the thickened emulsions during the *in vitro* lipid digestion. CE: conventional emulsion, NE: nanoemulsion, control: without thickener, ST: starch, and XG: xanthan gum.

in the mouth. However, the xanthan gum-based nanoemulsion did not show a considerable change in the particle size, and its distribution during oral processing remained unaltered. This may be explained by the formation of a structured network between small oil droplets and polymer chains that increased the resistance of oil droplets to coalesce under oral conditions.[51] In the case of starch-based emulsions, a breakdown of the swelling starch granules was also observed after the oral phase (Fig. 6) given the effect of enzyme hydrolysis of starch granules by α-amylase in the saliva.[52]

After the gastric phase, the digested emulsions (chyme) showed a particle size similar to or slightly higher than that in the mouth phase (Fig. 4), with a greater polydispersity of the particle size (Fig. 5). This behavior was verified by the micro-

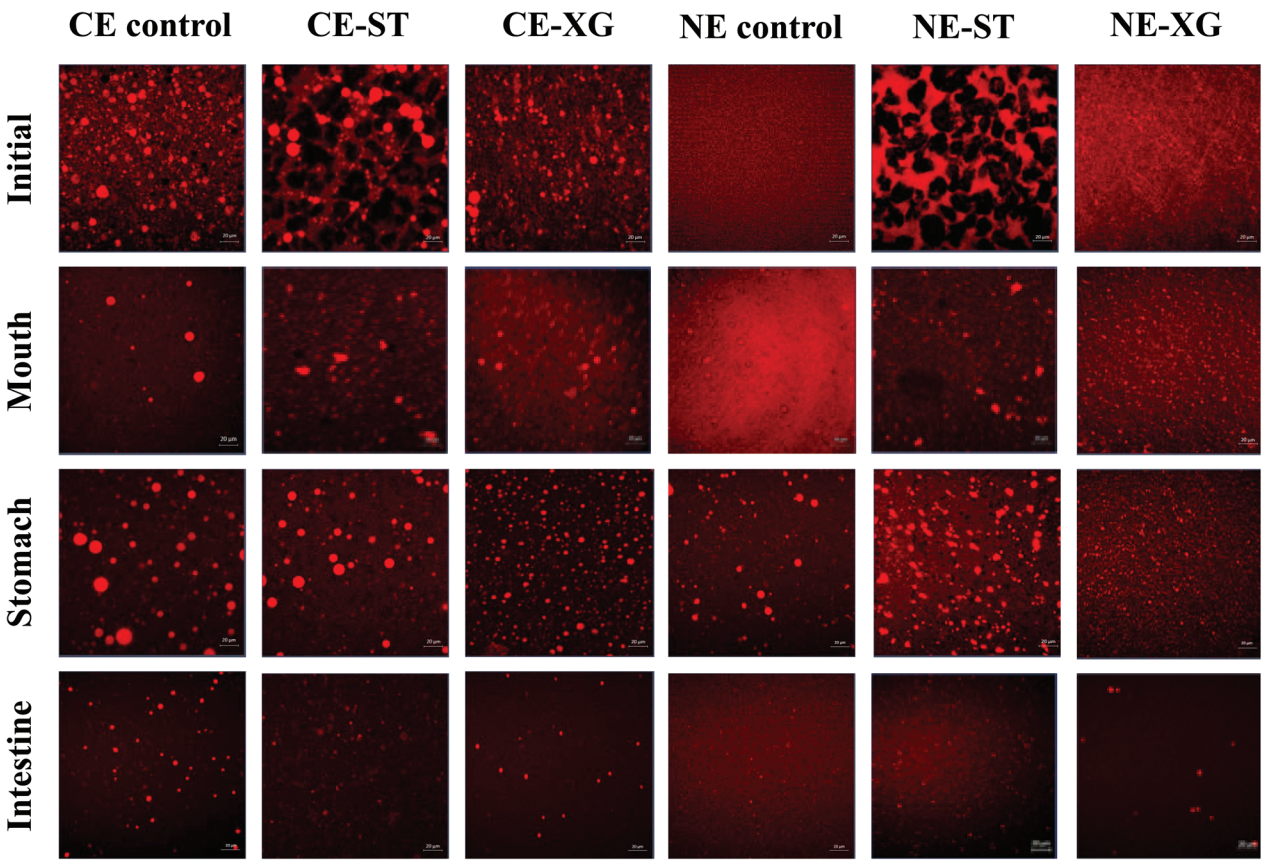

Fig. 6 Confocal micrographs of the thickened emulsions after the *in vitro* lipid digestion in each phase (mouth, stomach and intestine simulated conditions) and without digestion. CE: conventional emulsion, NE: nanoemulsion, control: without thickener, ST: starch, and XG: xanthan gum. Scale bars represent a length of 20 μm and the red regions represent lipids.

structure images (Fig. 6). An increase in the coalescence increased the wide peak of the particle size, due to the gastric conditions (high ionic strength and low pH). Regarding thickeners, the starch-based samples showed a higher particle size than xanthan gum-based samples after the stomach phase (Fig. 4 and 5), which was more noticeable for nanoemulsions. Differences between thickeners may be explained by the hydrolysis of starch in the mouth phase, since the breakdown of the structure could promote interactions between oil droplets and saliva components, which favors droplet aggregation[53] and increases the oil droplet coalescence under gastric conditions.[54] Instead, xanthan gum-based emulsions remained more stable because of the formation of a protective layer induced by this hydrocolloid around oil droplets that avoided their coalescence under gastric conditions.[29]

Regarding the intestinal phase, the chyle obtained showed a higher particle size than that obtained after the gastric phase, especially for control emulsions and xanthan gum-based emulsions and they showed a multimodal particle size distribution with an extensive range of oil droplet sizes that varied between 1–10 μm and 50–500 nm for conventional emulsions and nanoemulsions, respectively (Fig. 5). An increase of the particle size and the multimodal distribution may be attributed to the formation of micelles and vesicles containing digesta products (monoglycerides and free fatty acid–bile salt complex), and the coalescence of undigested drops,[41] which is also evidenced from the respective microstructure images (Fig. 6). In addition, the microstructure images showed a decrease in the amount of oil droplets in the chyle due mainly to lipase activity, which was more evident in nanoemulsions. This result is in agreement with the release of FFAs, since nanoemulsions showed the highest percentages of free fatty acids generated after the intestinal phase (Fig. 3 and Table 2).

Finally, the physical changes of the emulsions during their *in vitro* digestion could explain the differences found in the percentage of FFAs released. First, the extensive coalescence observed for the conventional emulsions through the *in vitro* digestive process affected lipid intestinal digestion, decreasing the FFA production. Second, the thickener addition altered lipid digestion decreasing the %FFAs released; however, xanthan gum can keep stable the particle size of nanoemulsions during the oral and gastric phases, avoiding the coalescence of oil droplets, which promotes the release of FFAs during the intestinal phase. Therefore, xanthan gum could be used as a thickening agent of nanoemulsions exerting a minor impact on their lipid bioaccessibility, which can be a useful tool for developing bioaccessible food products for elderly people.

4. Conclusions

Both the particle size and hydrocolloid type influence lipid bioaccessibility in O/W conventional emulsions and nanoemulsions, because of the structural changes that thickener-based emulsions undergo during *in vitro* digestion. The use of nanoemulsions increases the amount of free fatty acids (FFAs) released during intestinal digestion in comparison with conventional emulsions. The incorporation of different hydrocolloids (starch and xanthan gum) as thickening agents decreases the release of FFAs, but this behavior depends on the particle size. Xanthan gum-based nanoemulsions showed similar FFA production with respect to control nanoemulsions, with addition of no thickener. Therefore, the use of xanthan gum as a thickening agent of nanoemulsions represents a great alternative to starch because it generates less impact on lipid digestion. The results obtained from this study can be useful for designing emulsion-based food matrices with controlled nutrient delivery for populations with specific nutritional requirements such as elderly people.

Conflicts of interest

The authors declare no conflicts of interest.

Acknowledgements

This work was supported by ANID-PAI Grant No. 7916009, awarded to Carla Arancibia, and ANID-Doctoral grant No. 21170113, awarded to Natalia Riquelme.

References

1 K. Field and L. M. Duize, *J. Texture Stud.*, 2016, **47**, 266–276.
2 L. Laguna, M. M. Hetherington, J. Chen, G. Artigas and A. Sarkar, *Food Qual. Prefer.*, 2016, **53**, 47–56.
3 X. Song, D. Giacalone, S. M. Bølling-Johansen, M. Bom-Frøst and W. L. P. Bredie, *Trends Food Sci. Tech.*, 2016, **53**, 49–59.
4 T. Mann, R. Heuberger and H. Wong, *Aust. Dent. J.*, 2017, **58**, 200–206.
5 J. M. Aguilera and D. Park, *Trends Food Sci. Tech.*, 2016, **57**, 156–164.
6 C. Murphy and R. Vertrees, *Curr. Opin. Food Sci.*, 2017, **15**, 56–60.
7 V. Raikos and V. Ranawana, *Int. J. Food Sci. Technol.*, 2017, **52**, 68–80.
8 M. Artiga-Artigas, I. Odriozola-Serrano, G. Oms-Oliu and O. Martín-Belloso, in *Nanomaterials for food applications*, ed. A. López-Rubio, M. J. Fabra-Rovira, M. Martínez-Sanz and L. Gómez-Mascaraque, Elsevier, Netherlands, 2019, ch. 2, pp. 13–33.
9 D. J. McClements, *Biotechnol. Adv.*, 2020, **38**, 107287–107299.
10 D. J. McClements, *Food emulsions: Principles, practices, and techniques*, CRC press and Taylor & Francis Group, Boca Raton, 2015.
11 R. Zhang, Z. Zhang, H. Zhang, E. A. Decker and D. J. McClements, *Food Res. Int.*, 2015, **75**, 71–78.
12 R. Zhang and D. J. McClements, *Food Struct.*, 2016, **10**, 21–36.
13 Y. Li and D. J. McClements, *J. Agric. Food Chem.*, 2010, **58**, 8085–8092.
14 E. Troncoso, J. M. Aguilera and D. J. McClements, *J. Colloid Interface Sci.*, 2012, **382**, 110–116.
15 A. Khan, R. Carmona and M. Traube, *Clin. Geriatr. Med.*, 2014, **30**, 43–53.
16 L. Rofes, V. Arreola, R. Mukherjee, J. Swason and P. Clavé, *Aliment. Pharmacol. Ther.*, 2014, **39**, 1169–1179.
17 H. Cho and B. Yoo, *J Acad. Nutr. Dietetics*, 2015, **115**, 106–111.
18 C. D. Munialo, V. Kontogiorgos, S. R. Eusto and I. Nyambayo, *Int. J. Food Sci. Technol.*, 2020, **1**, 1–10.
19 M. Martínez, E. Troncoso, P. Robert, C. Quezada and R. Zúñiga, *Starch*, 2019, **71**, 1–2.
20 N. Garín, J. T. De Pourcq, R. Martín-Venegas, D. Cardona, I. Gich and M. A. Mangues, *Dysphagia*, 2014, **29**, 483–488.
21 K. Nishinari, M. Takemasa, T. Brenner, L. Su, Y. Fang, M. Hirashima, M. Yoshimura, Y. Nitta, H. Moritaka, M. Tomczynska-Mlekond, S. Mleko and Y. Michiwaki, *J. Texture Stud.*, 2016, **47**, 284–312.
22 S. Sukkar, N. Maggi, B. Travalca-Cupillo and C. Ruggiero, *Front. Nutr.*, 2018, **5**, 1–10.
23 J. M. Vieira, F. D. Oliveira, D. B. Salvaro, G. P. Maffezzolli, J. D. B. de Melo, A. A. Vicente and R. L. Cunha, *Curr. Res. Food Sci.*, 2020, **3**, 19–29.
24 M. Espert, A. Salvador and T. Sanz, *Food Hydrocolloids*, 2019, **95**, 454–461.
25 D. Fu, S. Deng, D. J. McClements, L. Zhou, L. Zou, J. Yi, C. Liu and W. Liu, *Food Hydrocolloids*, 2019, **89**, 80–89.
26 S. G. Kim and B. Yoo, *Int. J. Lang. Commun. Disord.*, 2015, **50**, 397–402.
27 E. Dickinson, *Food Hydrocolloids*, 2018, **78**, 2–14.
28 D. J. McClements, L. Bai and C. Chung, *Annu. Rev. Food Sci. Technol.*, 2017, **8**, 205–236.
29 Y. Chang and D. J. McClements, *Food Hydrocolloids*, 2016, **61**, 92–101.
30 X. Xu, Q. Sun and D. J. McClements, *Food Res. Int.*, 2020, **127**, 108768.
31 D. Qin, X. Yang, S. Gao, J. Yao and D. J. McClements, *J. Food Sci.*, 2016, **81**, 1636–1645.
32 C. Arancibia, M. Miranda, S. Matiacevich and E. Troncoso, *Food Hydrocolloids*, 2017, **73**, 243–254.
33 C. Arancibia, E. Costell and S. Bayarri, *J. Dairy Sci.*, 2011, **94**, 2245–2258.
34 A. Moret-Tatay, J. Rodríguez-García, E. Martí-Bonmatí, I. Hernando and M. J. Hernández, *Food Hydrocolloids*, 2015, **51**, 318–326.

35 G. Bortnowska, J. Balejko, G. Tokarczyk, A. Romanowska-Osuch and N. Krzemińska, *Food Hydrocolloids*, 2014, **36**, 229–237.
36 A. Brodkorb, L. Egger, M. Alminger, P. Alvito, R. Assunção, S. Ballance, T. Bohn, C. Bourlieu-Lacanal, R. Boutrou, F. Carrière, A. Clemente, M. Corredig, D. Dupont, C. Dufour, C. Edwards, M. Golding, S. Karakaya, B. Kirkhus, S. Le Feunteun, U. Lesmes, A. Macierzanka, A. R. Mackie, C. Martins, S. Marze, D. J. McClements, O. Ménard, M. Minekus, R. Portmann, C. N. Santos, I. Souchon, R. P. Singh, G. E. Vegarud, M. S. J. Wickham, W. Weitschies and I. Recio, *Nat. Protoc.*, 2019, **14**, 991–1014.
37 C. Qiu, M. Zhao and D. J. McClements, *Food Hydrocolloids*, 2015, **43**, 377–387.
38 Y. Cai, X. Deng, T. Liu, Q. Zhao and S. Chen, *Food Hydrocolloids*, 2018, **79**, 391–398.
39 X. Luo, Y. Zhou, L. Bai, F. Liu, R. Zhang, Z. Zhang, B. Zheng, Y. Deng and D. J. McClements, *Food Res. Int.*, 2017, **96**, 103–112.
40 D. J. McClements and S. Jafari, *Adv. Colloid Interface Sci.*, 2018, **251**, 55–79.
41 F. A. Bellesi, M. J. Martínez, V. M. Pizones Ruiz-Henestrosa and A. M. R. Pilosof, *Food Hydrocolloids*, 2016, **52**, 47–56.
42 E. Troncoso, J. M. Aguilera and D. J. McClements, *Food Hydrocolloids*, 2012, **27**, 355–363.
43 H. Majeed, J. Antoniou, J. Hategekimana, H. R. Sharif, J. Haider, F. Liu, B. Ali, L. Rong, J. Ma and F. Zhong, *Food Hydrocolloids*, 2016, **52**, 415–422.
44 R. Zhang, Z. Zhang, L. Zou, H. Xiao, G. Zhang, E. A. Decker, and D. J. McClements, Enhancement of carotenoid bioaccessibility from carrots using excipient emulsions: influence of particle size of digestible lipid droplets, *Food Funct.*, 2016, **7**, 93–103.
45 L. Salvia-Trujillo, B. Fumiaki, Y. Park and D. J. McClements, The influence of lipid droplet size on the oral bioavailability of vitamin D2 encapsulated in emulsions: an in vitro and in vivo study, *Food Funct.*, 2017, **8**, 767–777.
46 D. J. McClements, Enhanced delivery of lipophilic bioactive using emulsions: A review of major factors affecting vitamin, nutraceutical, and lipid bioaccessibility, *Food Funct.*, 2018, **9**, 22–41.
47 M. Espinal-Ruiz, F. Parada-Alfonso, L. P. Restrepo-Sánchez, C. E. Narváez-Cuenca and D. J. McClements, Impact of dietary fibers (methyl cellulose, chitosan, and pectin) on digestion of lipids under simulated gastrointestinal conditions, *Food Funct.*, 2014, **5**, 3083–3095.
48 L. Salvia-Trujillo, C. Qian, O. Martín-Belloso and D. J. McClements, *Food Chem.*, 2013, **141**, 1472–1480.
49 H. T. Cho, L. Salvia-Trujillo, J. Kim, Y. Park, H. Xiao and D. J. McClements, *Food Chem.*, 2014, **156**, 117–122.
50 S. Park, S. Mun and Y. R. Kim, *Food Res. Int.*, 2018, **105**, 440–445.
51 M. Espert, J. Borreani, I. Hernando, A. Quiles, T. Sanz and A. Salvador, *LWT–Food Sci. Technol.*, 2019, **112**, 108223.
52 A. C. Mosca and J. Chen, *Trends Food Sci. Technol.*, 2017, **66**, 125–134.
53 A. Sarkar, S. Zhang, M. Holmes and R. Ettelaie, *Adv. Colloid Interface Sci.*, 2019, **263**, 195–211.
54 L. Mao and S. Miao, *Food Eng. Rev.*, 2015, **7**, 439–451.

